A Rough Draft of My Thesis

Until I find the final, this is all I can share…

The Design and Construction of a Hybrid Electric Vehicle

by
Michael S. Civay

A THESIS

submitted to

The Physics Department
LINFIELD COLLEGE
McMinnville, Oregon

in partial fulfillment
of the requirements for the degree of

BACHELOR OF SCIENCE

MAY 2002

TABLE OF CONTENTS

I. Introduction

Our current dependence on the limited supply of fossil fuels and the growing worldwide concern over the hazardous effects of pollution have led to research in alternative methods of personal transportation.

Although purely electric vehicles (EV) seem like an ideal solution, present battery technology is not practical for common daily use of EVs. Although there are many exciting ideas in energy storage such as nickel-metal-hydride batteries, lithium-ion batteries, and fuel cells, they are still too expensive for practical use in a marketable consumer vehicle. Hybrid electric vehicle (HEV) technology is an effective method to reduce the harmful environmental impacts of the modern day automobile. Hybrid vehicles use a large battery pack as an energy storage buffer. The buffer stores normally wasted energy and gives it back when needed. Hybrid vehicles use this technology to reach levels of efficiency unobtainable by an automobile with a conventional internal combustion engine. It is for this reason that HEV technology will be the future of transportation.

II. Hybrid Electric Vehicle (HEV) Theory

Hybrid power systems were developed to compensate for shortcomings in battery technology. Batteries today can provide enough energy for short trips, and an onboard generator, powered by an internal combustion engine, could be installed and used for longer trips. Battery powered EVs re-charging using wall-plug electricity would provide optimal efficiency and emissions. With better batteries, we probably would not need hybrids at all, but after years of battery research, it seems that hybrids are most practical. Purely electric vehicles are only being used where fewer miles are traveled.

More efficient cars can greatly reduce the deterioration of air quality. Use of production HEVs will help reduce smog-forming pollutants over the current national average. Hybrids will never be true zero-emission vehicles, since they have an internal combustion engine. But according to gov pg the first hybrids on the market will cut emissions of global-warming pollutants by a third to a half, and later models may cut emissions by even more. HEVs have several advantages over conventional vehicles including regenerative braking, which helps minimize energy loss by recovering the energy normally lost slowing down or stopping a vehicle. Engines can be down sized to accommodate average load, not peak load, which reduces the engine's weight. Fuel efficiency is increased (hybrids consume significantly less fuel than vehicles powered by gasoline alone), and emissions are greatly decreased. HEVs can reduce dependency on fossil fuels since they are capable of running on alternative fuels.

A. Hybrid Power Units

Many configurations are possible for HEVs. A hybrid combines an energy storage system, a power unit, and a vehicle propulsion system. Options for hybrid power units include spark ignition engines, compression ignition direct injection engines, gas turbines, and fuel cells.

1. Spark Ignition (SI) Engine

A spark ignition (SI) engine runs on an Otto cycle—most gasoline engines run on a modified Otto cycle that uses a homogeneous air-fuel mixture, which is combined prior to entering the combustion chamber. Once in the combustion chamber, the mixture is compressed, then ignited using a spark plug. Limiting the amount of air allowed into the engine controls the SI engine. This is accomplished through the use of a throttle placed on the air intake (carburetor or throttle body).

Continual development over the last century of this technology has produced an engine that meets emissions and fuel economy standards. Due to advancements in technology, such as computer controls and reformulated gasoline, modern engines are more efficient and less polluting than engines built 20 years ago. The SI engine is the lowest cost engine because of the huge volume currently produced.

A few possible drawbacks to the SI engine include its difficulty in meeting future emissions and fuel economy standards at a reasonable cost. Technology has progressed and will enable the SI engine to meet present day standards, but as requirements become more stringent, the engine cost will continue to rise. To control an SI engine the air allowed into the engine is restricted using a throttling plate therefore the engine is constantly fighting to draw air past the throttle, which expends energy and lowers efficiency. Also SI engine is very complex and has many moving parts and there is friction loss between the parts. The losses through bearing friction and sliding friction further reduce the efficiency of the engine. And finally its limited compression ratio lowers its efficiency.

An SI engine was used in Cornell Universities' Slipstream HEV. An engine from a Geo Metro was fitted with a generator, this combination produced enough energy to allow the Slipstream travel more miles than any of their other HEVs.

2. Compression Ignition Direct Injection (CIDI) Engine

The compression-ignition direct-injection (CIDI) engine, (more commonly called the diesel engine), has the highest thermal efficiency of any internal combustion engine. Possible improvements include increasing the specific power, which is lower than the gasoline engine, decreasing the particulate matter and nitrogen oxides in the exhaust; and reducing the noise, vibration, and smell of the engine.

Recent advancements in high-speed automotive diesel engines, which address some of these shortcomings, have made them nearly ideal candidates for HEV applications. These advancements include high-pressure direct fuel injection, low oxides of nitrogen catalysts, and sophisticated electronic controls. With a thermal efficiency greater than 40% and well-understood maintenance, reliability, manufacturing, and operating characteristics, the high-speed CIDI engine shows great promise as a near-term hybrid power unit (HPU).

3. Fuel Cells

Fuel cells generate electricity through an electrochemical reaction that combines hydrogen with ambient air. Pure hydrogen or any fossil fuel that has been "reformed" can be used to produce a hydrogen-rich gas. Methanol is a common fuel choice. For the most part, the fuel cell's only emission is water vapor, giving it potential as the cleanest hybrid power unit alternative. Efficient, quiet, and reliable, fuel cells are predicted to demonstrate energy conversion efficiencies up to 50%, relatively high in comparison to the 20%-25% efficiency of standard gasoline engines.

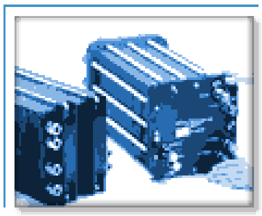

Figure 1.

The choice of fuel for a fuel-cell-powered HEV has important implications for required infrastructure, system accessories, efficiency, cost, and design. Although its viability has been well-proven in the space program, as well as in prototype vehicles developed by DOE and industry partners, very high capital costs, large size, long start-up times, and immature technologies make it a longer-term enabling technology for an HEV. Figure xx shows a compact fuel cell design that was sponsored by the DOE.

3. Gas Turbine Engine

The gas turbine engine runs on a Brayton cycle using a continuous combustion process. Figure xx shows a typical small gas turbine engine. Air is drawn into the engine through a mesh grill which helps protect the engine's fast moving innards from external objects. The air then passes through a rotating impeller which together with a ring of static vanes, forms the compressor section of the engine. The impeller is fitted with curved vanes at the intake area that guide the air into it, these are called rotating inlet guide vanes. As the air passes through the compressor it is accelerated outward at high speed and then slowed down in the ring of static vanes, this ring is known as the diffuser. The pressure of the air is raised to as much as four times atmospheric and is consequently heated.

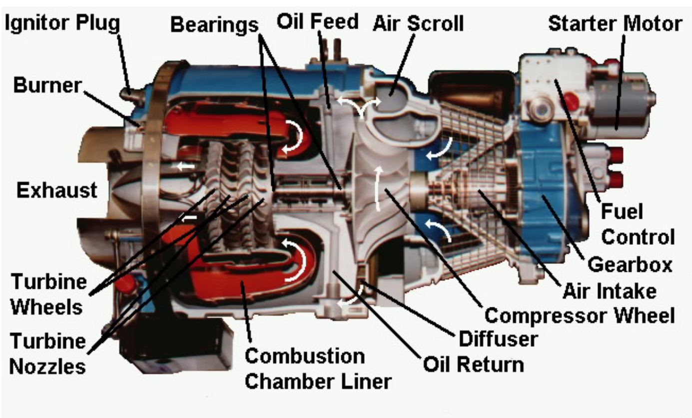

Figure 2.

When a turbine engine is directly coupled to a generator, it is often called a turbo generator or turbo alternator. The power output of a turbine is controlled through the amount of fuel injected into the burner. Many turbines have adjustable vanes and/or gearing to decrease fuel consumption during partial load conditions and to improve acceleration.

The turbine is light and simple, the only moving part of a simple turbine is the rotor. A turbine has no reciprocating motion, and consequently runs smoother than a reciprocating engine. A turbine will run on a variety of fuels - Any combustible fuel that can be injected into the airstream will burn in a turbine. A turbine has this flexibility because the continuous combustion is not heavily reliant on the combustion characteristics of the fuel. Because of their multi-fuel capability turbines produce low levels of emissions. A fuel, which burns completely and cleanly, can be used to reduce emissions.

The turbine engine has a few drawbacks, which have prevented its widespread use in automotive applications. Due to the complicated design turbine engines have high manufacturing costs. A turbine requires intercoolers, regenerators and/or reheaters to reach efficiencies comparable to current gasoline engines - This adds significant cost and complexity to a turbine engine. Turbines are noisy, and special sound deadening enclosures need to be made to reduce the 120db out put to a more reasonable level.

B. Energy Storage

Hybrid vehicles use a large battery pack as an energy storage buffer. The buffer stores normally wasted energy and gives it back when needed. Hybrid vehicles use this technology to reach levels of efficiency unobtainable by an automobile with a conventional internal combustion engine alone. The primary options for energy storage include batteries, ultra-capacitors, and flywheels. Currently batteries are the most common energy storage choice however, research is still being done in other energy storage areas.

1. Flywheels

Although flywheels are currently being used in some bus applications, more work needs to be done to make flywheels safe and effective for personal HEV applications. Current flywheels are still very complex, heavy, and large for personal vehicles. In addition, there are some concerns regarding the safety of a device that spins mass at high speeds.

A flywheel for HEV applications stores kinetic energy within a rapidly spinning wheel-like rotor or disk. Ultimately, flywheels could store amounts of energy comparable to batteries. They contain no acids or other potentially hazardous materials. Flywheels are not affected by temperature extremes, as most batteries are.

Flywheels have been used in various forms for centuries, and have a long history of use in automotive applications. Early cars used a hand crank connected to a flywheel to start the engine, and all of today's internal combustion engines use flywheels to store energy and deliver a smooth flow of power from the abrupt power pulses of the engine.

Modern flywheels employ a high-strength composite rotor, which rotates in a vacuum chamber to minimize aerodynamic losses. A motor/generator is mounted on the rotor's shaft both to spin the rotor up to speed (charging) and to convert the rotor's kinetic energy to electrical energy (discharging). A high-strength containment structure houses the rotating elements and low-energy-loss bearings stabilize the shaft. See figure xx for a view of a modern flywheel. Interface

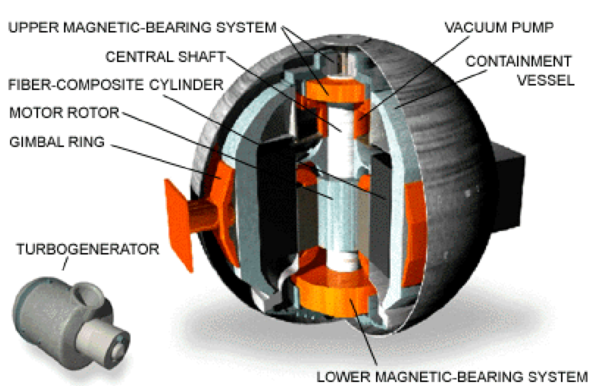

. *Figure 3.*

electronics are needed to convert the alternating current to direct current, condition the power, and monitor and control the flywheel.

Flywheels could be used in HEVs in several ways, and all of them exploit the ability to deliver very high power pulses. One idea combines a flywheel with a standard engine, providing a power assist. Another concept employs a flywheel to load-level chemical batteries. Still another uses a large or multiple flywheels to replace chemical batteries entirely. For flywheels to have success in HEVs, they would need to provide higher energy densities than what is now available.

2. Ultra-capacitors

Ultra-capacitors are higher specific energy and power versions of electrolytic capacitors, which store energy as an electrostatic charge. They are electrochemical systems that store energy in a polarized liquid layer at the interface between an ionically conducting electrolyte and a conducting electrode. Energy storage capacity increases by increasing the surface area of the interface. Ultra-capacitors are being developed as primary energy devices for power assist during times of heavy drain, such as during acceleration and hill climbing, as well as recovery of braking energy. Current research and development aims to create ultra-capacitors with capabilities of Wh/kg and 1,000 W/kg. Additional electronics are required to maintain a constant voltage, because voltage drops as energy is discharged.

3. Batteries

Lead acid batteries are used currently in many electric vehicles and can be designed to be high power, inexpensive, safe, and reliable. Recycling programs are available for them. But low specific energy, poor cold temperature performance, and short calendar and cycle life are still impediments to their use. Advanced high-power lead acid batteries are being developed for HEV applications as can be seen in figure xx.

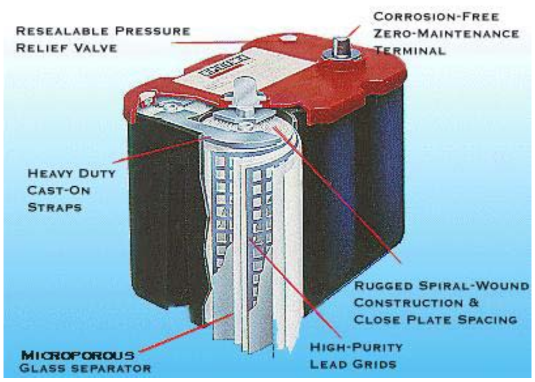

Figure 4.

Although nickel-cadmium batteries, used in many electronic consumer products, have higher specific energy and better life cycle than lead acid batteries, they do not deliver sufficient power and are not considered for HEV applications.

Nickel-metal hydride batteries, which are used routinely in computer and medical equipment, can offer reasonable specific energy and specific power capabilities. Their components are recyclable, but a recycling structure is not yet in place. Nickel-metal hydride batteries have a much longer life cycle than lead acid batteries and are safe and abuse-tolerant. These batteries have been used successfully in production Evs and recently in low-volume production HEVs. The main challenges with nickel-metal hydride batteries are their high cost, high self-discharge and heat generation at high temperatures, the need to control losses of hydrogen, and their low cell efficiency.

The lithium ion batteries are rapidly penetrating into laptop and cell-phone markets because of their high specific energy. They also have high specific power, high-energy efficiency, good high-temperature performance, and low self-discharge. Components of lithium ion batteries could also be recycled. These characteristics make lithium ion batteries suitable for HEV applications. However, to make them commercially viable for HEVs, further development is needed similar to those for the EV-design versions including improvement in calendar and cycle life, higher degree of cell and battery safety, abuse tolerance, and acceptable cost.

Lithium polymer batteries with high specific energy, initially developed for EV applications, also have the potential to provide high specific power for HEV applications. The other key characteristics of the lithium polymer are safety and good cycle and calendar life. The battery could be commercially viable if the cost is lowered and higher specific power batteries are developed. Batteries are an essential component of the HEVs currently under development. Although a few production HEVs with advanced batteries have been introduced in the market, no current battery technology has demonstrated an economical, acceptable combination of power, energy efficiency, and life cycle for high-volume production vehicles. The Partnership for a New Generation of Vehicles program has established technical targets for the program's hybrid battery development efforts for power-assist and dual-mode HEVs.

Desirable attributes of high-power batteries for HEV applications are high-peak and pulse-specific power, high specific energy at pulse power, a high charge acceptance to maximize regenerative braking utilization, and long calendar and cycle life.

Developing methods/designs to balance the packs electrically and thermally, developing accurate techniques to determine a battery's state of charge, developing abuse-tolerant batteries, and recycleability are additional technical challenges.

C. Propulsion

Propulsion can come entirely from an electric motor, such as in a series configuration, or the engine might provide direct mechanical input to the vehicle propulsion system in a parallel configuration system.

A hybrid's efficiency and emissions depend on the particular combination of subsystems, how these subsystems are integrated into a complete system, and the control strategy that integrates the subsystems. A hydrogen fuel cell hybrid, for example, would produce only water as a by-product and run at greater overall efficiency than a battery-electric vehicle that uses wall-plug electricity.

1. *Series Configuration*

An HEV with a series configuration uses the heat engine or fuel cell with a generator to produce electricity for the battery pack and electric motor. Series HEVs have no mechanical connection between the hybrid power unit and the wheels; this means that all motive power is transferred from chemical energy to mechanical energy, to electrical energy, and back to mechanical energy to drive the wheels. Some benefits of a series configuration include that the engine never idles, which reduces vehicle emissions. The engine drives a generator to run at optimum performance. Its design allows for a variety of options when mounting the engine and vehicle components. And some series hybrids do not need a transmission, which reduces weight and complexity.

The downside is that series HEVs require larger, and therefore, heavier battery packs than parallel vehicles. More batteries are needed in series applications since all the energy that propels the vehicle must come from the batteries, while a parallel runs a combination running both from combustable fuel and batteries, as I will discuss next.

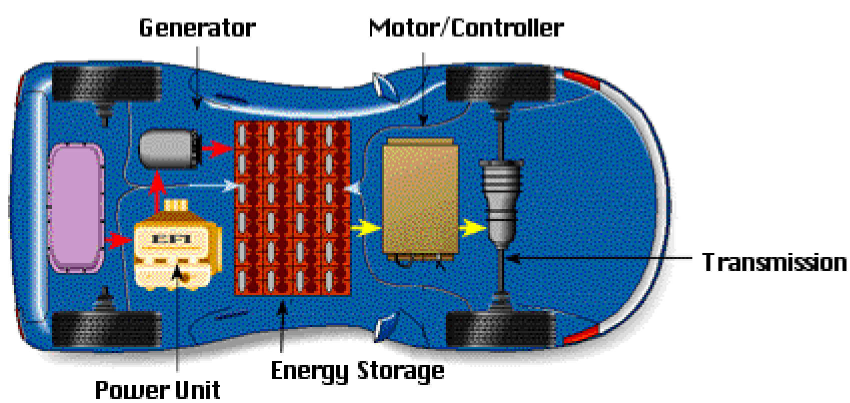

Figure 6.

2. Parallel Configuration

An HEV with a parallel configuration has a direct mechanical connection between the APU and the wheels, as in a conventional vehicle, but also has an electric motor that drives the wheels. For example, a parallel vehicle could use the power created from an internal combustion engine for highway driving and the power from the electric motor for accelerating.

Some benefits of a parallel configuration are that the vehicle has more power because both the engine and the motor supply power simultaneously.

Most parallel vehicles do not need a separate generator because the motor regenerates the batteries. Because the power is directly coupled to the road, it can be more efficient than a series configuration. Two HEVs presently being sold in the US are the Honda Insight and the Toyota Prius, both cars use a form of a parallel configuration.

Drawbacks to a parallel confguration include the increased complexity in electronic control circuitry. The system to link both electrical and mechanical motors to provide power to the road

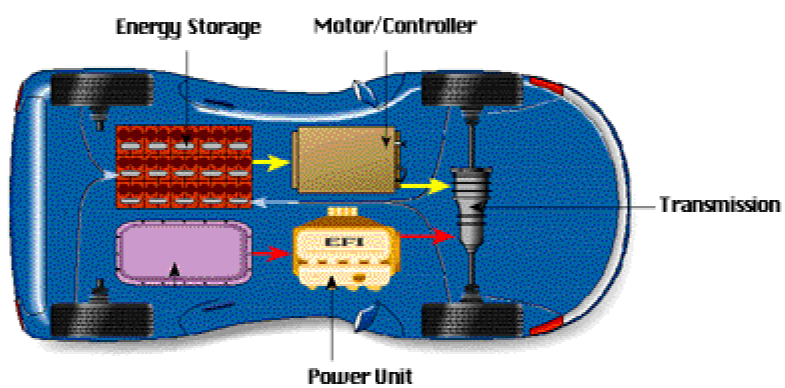

Figure 7.

3. DC Motor

In an HEV, an electric traction motor converts electrical energy from the energy storage unit to mechanical energy that drives the wheels of the vehicle. Unlike a traditional vehicle, where the engine must "ramp up" before full torque can be provided, an electric motor provides full torque at low speeds. This characteristic gives the vehicle excellent "off the line" acceleration.

Important characteristics of an HEV motor include good drive control and fault tolerance, as well as low noise and high efficiency. Other characteristics include flexibility in relation to voltage fluctuations and acceptable mass production costs. Up and coming technologies for HEV applications include the permanent magnet, AC induction, and switched reluctance motors

The motor in my HEV is a series wound DC motor. This means that there aren't any magnets in the motor, but instead a field winding of wire that becomes an electro-magnet when current flows through it. A series motor means that the same current that flows through the rest of the motor (armature) also flows through the field windings. This means heavy-duty wire and connections for every aspect of the motor to withstand the high current. The motor is wired in the diagram above so that the negative output side of the controller goes into the field winding (S1), the field winding output is shorted to the armature (S2-A2), and the other armature connection (A1) is hooked to the positive side of our 144 volts Motor.

4. Controller

The controller is a Pulse Width Modulation (PWM) controller that is typical in most HEVs. The controller sits like a switch between the negative side of the batteries and the negative contact of the motor. The positive cable is hooked to the controller as well, but for reasons other than direct control (spike suppression, etc.) The controller will also monitor its self for over current and overheating conditions, shutting down temporarily if needed. There are also safety interlocks to make sure everything is hooked up right, and some controllers will even monitor other aspects of the motor. A cooling fan is necessary that will be mounted below the controller to help keep it cool.

4. Ignition Switch

The ignition switch has lost some importance. The whole concept of "starting" is no longer relevant. The EV merely needs an on/off switch and the ignition switch is as good of candidate as any. Some of the newer, commercial EVs (like the GM Impact) don't even have an ignition switch. They use a little electronic keypad for entering in a code to unlock and turn on the EV.

5. Circuit Breaker

As a master on/off switch for all of the EV's drive circuitry I decided to use a fork lift emergency cut of switch. That way I can completely turn off the circuit when doing work, or it can be used to quickly shutdown in an emergency by kicking a large lever.

6. PotBox (Accelerator)

This is what the accelerator cable hooks to now. The box translates foot pressure into a variable resistance to let the controller know how fast you want to go. In addition there is a safety switch inside that helps prevent starting the EV with the gas pedal is fully compressed.

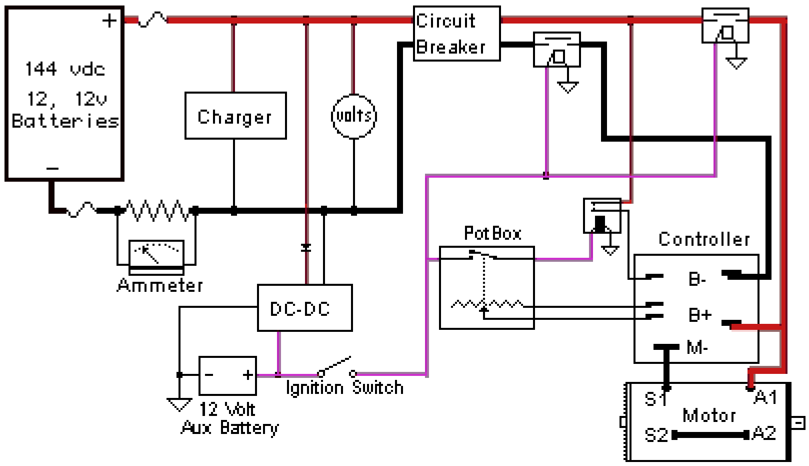

Figure 8.

This is a rough combination of schematic and block diagram, Red is 120vdc positive; purple is 12vdc positive, while black is ground (the 120vdc and 12vdc grounds ARE separate). The heavy, main current flow is indicated by the wider lines. Also, wires, which cross each other, are not connected unless a junction at the crossing can be seen.

D. Future of HEVs

Auto manufacturers are making these HEVs with comparable performance, safety, and cost because they know that these three elements are most important to consumers. And by combining gasoline with electric power, hybrids will have the same or greater range than traditional combustion engines. The HEV is able to operate approximately two times more efficiently than conventional vehicles. Honda's Insight can go 700 miles on a single tank of gas. The Toyota Prius can go about 500 miles. For the driver, hybrids offer similar or better performance than conventional vehicles. More important, because such performance is available now, hybrids are a practical way for consumers to choose a cleaner drive today.

III. Automotive Design Theory

I chose to design a car instead of modifying an existing design. This is because current cars are heavy and are designed around very different perimeters to that of my own. My goal is to build a lighter, and thereby more efficient test platform for the concept of a turbine auxiliary power unit on an electric vehicle. The frame must support the turbine, battery weight, electric motor, and safely contain the driver. It also must be maneuverable and durable. With these perimeters in mind I began to design the frame.

1. Instant center

First I studied dimensions of existing automobiles, and the components, which I could adapt to my own car. I started the design with track width and wheel size, to bring the location available for the lower ball joint. The upper ball (UBJ) joint is located either via kingpin angle requirements or scrub radius requirements. Increasing the distance between the upper and lower ball joints (LBJ) reduces the loads on the control arms, and the suspension components. With upper and lower ball joint locations established, the tie rod outer point should also be set. The front view swing arm (fvsa)instant center is determined by the desired roll center height and roll camber. The desired roll camber sets the front view swing arm length as follows:

fvsa=(t/2)/(1-roll camber)

where t= track width

Roll camber = wheel camber angle/chassis roll angle (with both measured relative to the road)

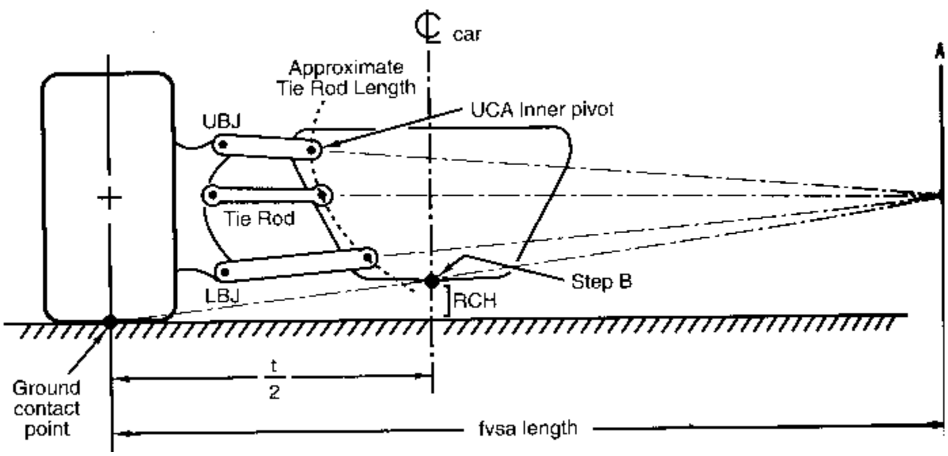

Figure 9.

The front view instant center height is set by projecting a line from the tire center ground contact patch through the desired roll center height. The instant center must lie on this line. Now we can project lines from both ball joints to the instant center. These become the centerlines of the upper and lower control arm planes as projected into the vertical plane through the wheel center. Packaging requirements will establish the length of the lower control arm but it should be as long as possible. The length of the upper control arm in relation to the lower arm adjusts the shape of the camber curve. If they are the same lengths the camber versus wheel travel curve will be a straight line. If the upper is longer than the lower, the curve will be convex with its curvature toward positive camber. If the upper is shorter than the lower, the curve will be concave toward negative camber. As the upper is made progressively shorter, the curvature increases. To finish in the front view geometry, the tie rod and rack and location should be roughed in. Projecting a line through the tie rod outer point (est. ch19 on steering) and the front view instant center does this. The correct tie rod length is the established for a linear ride toe curve. This length will be modified after the side view geometry is completed, but doing it now is a good idea to help plan a realistic arc location

3. Roll Center

Next it is important to determine the roll center height. The roll center establishes the force coupling point between the un-sprung and sprung masses. When a car corners, the centrifugal force at the center of gravity is reacted by the tires; the lateral force at the CG can be translated to the roll center if the appropriate force and moment (about the roll center) are shown. The higher the roll center the smaller the rolling moment about the roll centers (which must be resisted by the springs) the lower the roll center the larger the rolling moment. You will also notice that with higher roll centers the lateral force acting at the roll center is higher off the ground. This lateral force multiplied by the distance to the ground can be called the non-rolling overturning moment. So roll center heights are trading off the relative effects of the rolling and non-rolling moments. The Roll center height is found by projecting a line from the center of the tire-ground contact patch through the front view instant center as shown in figure 17.7. This is repeated for each side of the car. Where these two lines intersect is the roll center of the sprung mass of the car, relative to the ground.

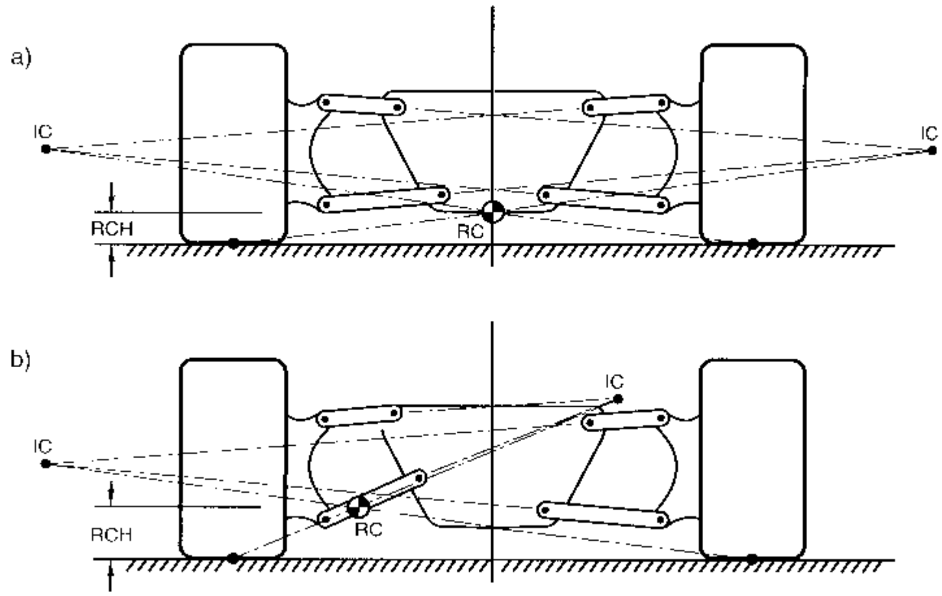

Figure 10.

The roll center location is controlled by the instant center heights above or below ground, the distance away from the tire that the instant center is placed, and whether the instant center is inboard or outboard the tire contact patch.

There is another factor in establishing the desired roll center height, and this is the horizontal-vertical coupling effect. If the roll center is above ground level the lateral force from the tire generates a moment about the instant center (IC). This moment pushes the wheel down and lifts the sprung mass; it is called jacking. See fig xx. If the roll center is below the ground level (possible with SLA suspension only) then the force will push the sprung mass down. In either case the sprung mass will have a vertical deflection due to a lateral force. An alternate way to analyze this is with the use of a force triangle. In Figure xxb the total force at the contact patch is drawn to its reaction point at the instant center and the lateral and vertical components are indicated; the vertical components in the case shown will lift the sprung mass.

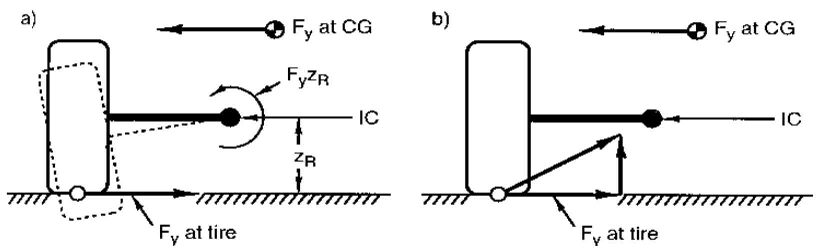

Figure 11.

4. Raising Rate Design Theory

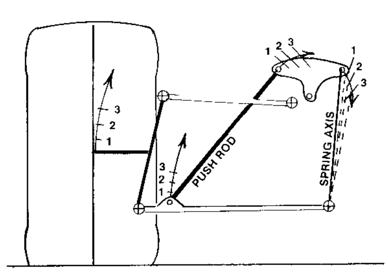

. *Figure 11.*

Next the type of suspension design had to be chosen. A "Raising Rate" suspension system was chosen as it is both very adjustable and individual parts can be machined and replaced easily. By a push rod and a bell crank altering the length of the rod will alter the geometry of the system, changing both the rate of increase in the wheel rate and the zero point of the rate of change curve. The length of the operating rod is a critical part of the design parameters of the suspension system

B. Suspension Springs

1. Coil Springs

To counter the force imparted by the push rod coil springs will be used, I chose them are relatively light, adjustable and are simple to maintain. Coil spring utilizes the elastic properties of a wire in torsion to produce a rectilinear spring rate; they are the most widely used spring types in independent suspensions for automobiles. The most common shape is the helix in which the mean diameter of the coil is constant; variation range from tapered coils (in which the mean diameter varies) to coils with varying wire diameter. Coil springs can be designed for use in compression or extension. Helical coil springs were chosen and they will be used in compression. Figure 21.3 gives the nomenclature for the helical coil springs and typical ends that are used for compression springs.

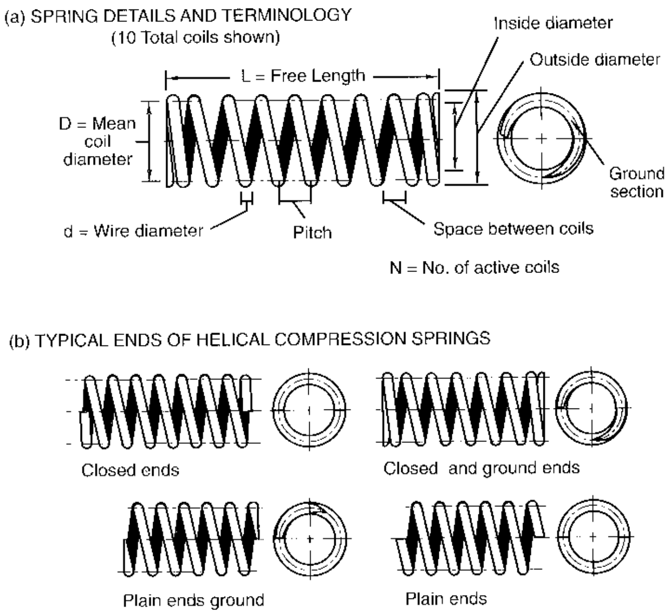

Figure 21.3 Helical coil compression springs (Ref. 6).

A. Maximum Stress

The maximum shear, f, in a coil spring with load, w, is given by

$f=8DW/PId^3=2.55DW/d^3$

The maximum stress given by this equation is designated the "uncorrected" stress; it does not take into account stresses caused by the curvature of the wire into a coil and other factors. A multiplying factor, called the Whal factor, must be used to increase the result found in the right hand side of the equation above. This factor is a nonlinear (and inverse) function of the ration of mean diameter to wire diameter.

B. Spring rate:

The spring rate (pounds of load per unit deflection) is given by

S= Gd^/8D^3N=W/X, lb/in

C. Steering Systems

Next the steering geometry must be determined. Tire scrub in a turn is avoided by arranging the steering linkage so that the inside front wheel is steered through a greater arc than the outside one.

1. Ackerman Steering Geometry

For low acceleration usage (streetcars) it is common to use Ackerman geometry. This geometry ensures that all wheels roll freely with no slip angles because the wheels are steered to track a common turn center. Notice that at low speeds all wheels are on a significantly different radius, the inside front wheel must steer more that the outer front wheel. A reasonable approximation to this geometry may be made as shown in figure below:

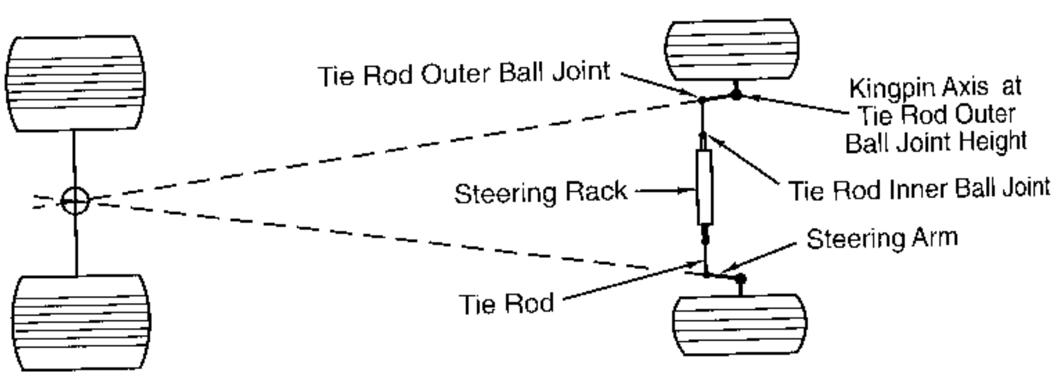

Figure 13.

2. Rack and Pinion Steering

In modern cars it is common to assist the steering with a rack and pinion. Rack-and-pinion gear sets convert rotary motion at the steering wheel to linear motion at the inner tie rod ball joint. The steering is calculated using the rack c-factor and the steering arm length (as measured from the outer ball joint to the kingpin axis).

V. Construction

The frame was built out of an aircraft grade T6061 aluminum for several reasons. First, aluminum is light and strong, see figure xx for T6061 specifications. In areas of the frame such as the front and rear suspension sections where more strength is needed, thicker .5″ T beams were used as braces. A second property that influenced the decision to use aluminum is that it is relatively easy to machine. Also, when polished or anodized, aluminum is very durable and does not rust or corrode. Finally aluminum was chosen, as it was attainable for the relatively low price of $1.00 a pound in remnants.

Although thin walled aluminum is difficult to weld, it can be successfully bonded and bolted together. In general, welding weakens the aluminum and only through a skillful process of re-heating around the joint does it regain some of its initial strength. This process is very time consuming and would not be practical in large-scale production. I also lack the skills to perform such welding. Bonding and bolting the aluminum sections together as a production method is used by Lotus in it new Elise model. This frame begins with bent, extruded sections, which are intern bonded together with an epoxy. Further additions are then bolted to the structure. Extruding bent rails is a new technology and one I do not have access to. Aluminum cannot be bent without weakening it so the frame had to be designed with no bends.

The frames of older cars usually consist of two main rails running parallel down the center of the frame the body would be bolted to the rails and passengers would sit on top of this frame wrapped inside of the body. This design was improved in 1963 with the corvette stingray, which placed the passengers inside of the frame, between the two rails. This configuration allowed for a lower roll center, better handling, and a more aerodynamic body. Most new cars do away with the old rail frames as they carry the stresses of the road throughout the body. This newer form is called a space frame, and its design incorporates many of the features held in aerospace engineering, that is by using thin folded metal as supports to carry the stresses of the road in the skin of the body, in essence incorporating the body as a frame. This design saves weight as the space frame eliminates redundant structural material. These cars also prove to be better in crash tests as the force of the cash is spread thought the car to calculated breaking points. With these lessons in mind the frame was designed accordingly.

The design restrictions of the inability to bend the metal or weld created difficulty I the frame design. If the driver is left to sit on top of the frame he would loose response and feeling of the road, also the weight of the driver should be centrally located to reduce the roll center, as was discussed earlier. these two factors contribute to a loss of handling. As the frame rails could not bent around two people as the Lotus and Corvette, a one- person design had to be considered where the driver sits between the straight rails. Next the uni-body design of thin walled metal meshing the body and frame together was considered. And so by running four 3″ by 3″ thin walled aluminum rails, which constitute the structure for both the suspension and the body, a space frame type of design had begun, (see fig xx). With the driver sitting well inside of the frame he finds himself in a safer position. This structure also provides the strength needed to carry the eight 50 pound lead acid batteries. It was a goal to incorporate all necessary all necessary structures, such as battery, driver, motor, and suspension containment into the strength of the frame.

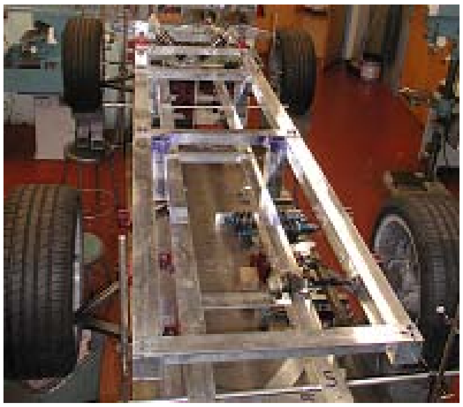

Figure xx.

Frame

While round tubing of a similar cross sectional area would prove to be stronger than the square tubing I chose, the square tubing has a flat surface to mate the other parts with, providing a larger area for epoxy bonding and bolting. I considered press fitting the frame together as this proved to be a very effective method of joining aluminum in the passive dynamic walking machine I built last summer. But the tolerances for tight press fitting are very small, and so fittings would require a lot of time to produce, also fittings would make the frame quite heavy. The final deciding factor to the square tubing is that it was all that was available for $1.00 a pound.

The frame was designed with four 3″ by 3″ extruded aluminum beams, each 96″ long. The upper beams were 3″ wider on each side than the lower beam; this was done to allow for smaller upper A-arms, which is a requirement for double A-arm suspension systems. As the gap on each side was 3″ the same 3″ by 3″ beam material was used to link the upper and lower sections. The vertical gap between upper and lower rails is x″ this again was dictated by suspension design as the separation between A-arms attributes to the handling of the car. This is discussed further in section xx. Every connection in the frame rails was supported by inserting 1″ by 1″ aluminum square stock spacers, which fitted snugly inside the frame rails.

Before the frame was to be assembled all parts were polished. Polishing seals the outer layer of the aluminum from corrosion. Parts that were difficult to polish were anodized. Anodizing is important where the aluminum comes in contact with steel, and as all the suspension joints are held together with steel bolts and hold steel pins all suspension components were anodized. Every bolt used in the suspension was of grade 8. Where the bolts went though the frame, 2 7/8″ by 2″by 2″ squares were inserted to prevent the walls from collapsing under the stress of the bolts. Also by inserting the spacers the force exerted on the rail by the joint is distributed more evenly across that section of the frame see section xx for a stress analysis a joint supported and un-supported by a spacer.

Battery Trays

Figure xx.

Battery trays were constructed out of 1″ by 2″ steel bars which were TIG welded together, these trays were bolted on to the upper frame rails to the ends of the existing grade 8 bolts which were used to fix the T shaped aluminum cross supports see fig. xx. The bottom of the tray was then fixed to the lower frame rails with 1″ by 1″ aluminum spanning bars see fig. xx. This arrangement provides support to the upper and lower frame, and provides a safe and accessible location to store the batteries. In section xx a stress analysis is performed in this section of the car to analyze its benefits to the frames overall strength.

Electric motor mount

The electric motor mount was designed to brace the 8″ Advanced DC electric motor and to provide lateral support to the frame. The mount was constructed out of both 1″ by 1″ steel square stock and 1″ by 3″ rectangular stock, as well as 4 sheets of .25″ thickness steel sheet see. All parts were either TIG or MIG welded and the finished mount was coated with a corrosion resistant paint to seal the metal. The square and rectangular stock constituted the frame of the mount while the sheet was used to mate against the face of the electric motor see figure xx. The face of the electric motor has pre-threaded mounting holes for bolts and so a larger horizontal hole was made in the steel mounting sheet in order to provide adjustability in the vertical mounting of the motor. This space allows for some belt adjustment, further belt adjustment is taken care of by a tension pulley see fig. xx. This pulley is applies pressure against the belt, it connected to the frame by a spring-loaded arm, and the tension of the belt is there by adjusted by rotating a bolt, which rotates the spring, which then applies greater pressure on the belt.

Suspension

I decided upon a double A-arm structure with a raising rate suspension system. Individual coil springs were used to support each wheel providing an independent 4-wheel design.   This system provides very good handling while offering simple adjustabliliy.

A-arms

Lower A-arms were constructed with 1.5″ by 1.5″ square stock steel tubing, while upper A-arms were built with smaller 1″ by 1″ tubing as much less stress is held in them, see analysis section xx. The tubing was then TIG and MIG welded together to produce the finished forms seen in figure xx. The A-arms were connected to the frame with high quality NMB rod ends to the frame. Aluminum braces were machined and anodized to join the rod end to the frame. Each brace was precisely reamed to provide a snug fit for a ¾ “steel pin, which slid though both rod end and brace. The braces were then mounted to the frame with x mm. grade 8 bolts, which were threaded into the pre-tapped braces and then secured with an additional nut. The front A-arms were then connected to the knuckles and then the wheels via rod ends and adapters. The knuckles were from a 2000 BMW 3 series and were originally built for a strut suspension system, so adapters had to be made. For the upper A-arms aluminum blocks were machined which were tapped out in three places, grade 8 bolts were then threaded though existing holes in the knuckles and into the adapters to a tight fit as seen in figure xx. The lower A-Arms was connected by running a ¾" grade 8 bolt though a vertical hole in the bottom of the knuckle though the lower rod end. Stainless steel spacers were then placed between the knuckle and the rod end to provide a greater separation between the rod ends. This separation is called the kingpin inclination, the effects of which were discussed in Section III.A.2, titled Instant center. The rear A-arms were joined differently, they were bolted directly to existing joints in the rear knuckles see figure xx.

Push Rods

The push rods were made from solid, extruded aluminum xx" diameter round stock. The ends were drilled and tapped for the ¼" rod ends. The rod ends are screwed into the bars and are tightened with jam nuts, see figure xx. The rod ends were connected between the lower A-arms and the bell cranks. For the front push rod is bolted though two steel tabs welded in the center of the front lower A-arms see figure xx. The upper part of the front push rods is bolted between two aluminum plates constituting the bell crank. Stainless steel spaces are placed on either end between the rod end and the steel tab. Spacers were used in all links to ensure a snug fit and allow for the degree of motion needed in the rod end during suspension travel. The upper rear rod ends were mounted similarly as the upper front rod ends, however for the lower rear rod ends, as there is an axle down the center

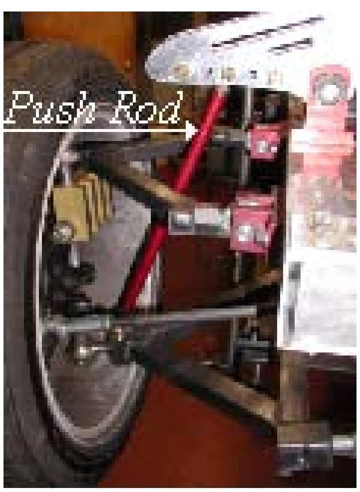

Figure xx.

of the rear A-arms and the push rod had to be mounted elsewhere. The push rod was mounted behind the axle as seen in figure xx. A stub was welded onto the rear knuckles and the push rod was bolted to it. The rear knuckles were also from a 2000 BMW 3 series and were originally built for struts. As a result a large stabilizer bar which was a part of the solid cast steel knuckle had to be removed see fig xx.

Bell Cranks

Each bell crank was made of two ½" aluminum sheets with several holes to adjust the angle and height of the push rod see figure xx. As the push rod is bolted in different positions there is a trade-off in the stiffness of the ride and the ride height. This trade-off is analyzed in section xx.

Coil Springs

Coil spring shocks, "coil-overs" were chosen for their relative simplicity and easy adjustment. The front coil-overs are xx" by xx" spax racing brand, with steel bodies, they are adjusted by tightening a collar around the body of the shock which compresses the spring. The rear coil-overs are AFCO racing brand and have aluminum bodies, they are adjustable also. Through adjustments to the coil-overs and to the push rod location on the bell crank, as well as the spacers between the upper and lower A-

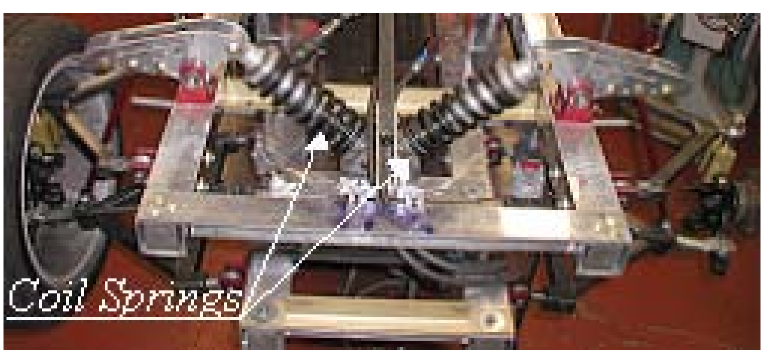

Figure xx. arms, the ride characteristics of the car are altered and fine-tuned. The upper body of each coil- over was bolted to the bellcrank while the lower section was mounted in the center of the lower frame rails. In figure xx. the front coil-over arraignment can be seen. Two mounts were machined out of xx″ by xx″ aluminum blocks. These blocks are slightly adjustable and lock the coil-overs in place to the desired geometry. These blocks are mounted on to a xx″ by xx″ aluminum bar that spans the lower frame rails. This bar provides reactionary support for the coil-overs when compressed. An analysis of this system can be seen in section xx.

Body Structure

The skin of the body is Alclad aluminum of .020″ thickness, this is the same aluminum that is used on aircraft. The Alclad is stretched and rived to thin xx″ by xx″ rectangular bands that are first bent to the correct curve then bolted to the frame rails. A compound curve was achieved in the rear section by angling the skeleton bands to correspond the slope of the skin and then decreasing the size of the band consecutively towards the back of the car, the effect can be seen in figure xx. Before any piece of the Alclad was cut, cardboard pieces were used to get the correct measurements. These cardboard pieces served as a template and the Alclad was traced and cut to match. After each piece was cut, holes were punched in the skin and drilled into the skeleton bands. The skin was next riveted to the skeleton. Riveting provides a strong connection and can easily be removed with a drill and as the rivets are also aluminum they are light which leads to an overall light body capable of supporting stress loads.

Steering

A rack and pinion was used to the control steering. In order to provide more space for the driver's legs the left and right front knuckles were switched. Switching the knuckles moved the steering arms out in front and moved the rack and pinion further forward. Steering arms are generally placed facing backwards and not as I have placed them as they are less susceptible to moving when bumped. The rack and pinion I used has a sharp 30-degree angle coming off it; this is common in cars as he driver generally sits to the right of the rack. The diver in this case is actually sitting on the left and so adjustments had to be made. Several aluminum universal joints from the steering column were removed from late model BMW cars and were used to link up the steering wheel and the rack. The steering wheel was mounted to a 5" diameter solid round stock of aluminum that was turned down on a lathe. Holes were then tapped to fit the steering wheel see figure xx for a view of the column. The end of the column was cut out and a universal joint was bolted in. The column was supported by an adjustable "pill box" style bearing mount. A brace was made to hold the universal joints in place, the linkage can be seen in figure xx.

Braking

The existing 4 wheel disk brakes from the BMW were used; a universal master cylinder and pedal assembly pushed the hydraulic fluid to compress the brake calipers on the disks.

Gas Turbine Testing

The condition of an experimental auxiliary power unit, or apu, was analyzed through a series of studies involving its components and the principles under which it operates. The apu was found to be in operational condition and test runs were preformed.

Figure xx.

This auxiliary power unit (apu) has a “can combuster” style chamber where combustion takes place. Exhaust from the combustion then impinges upon the turbine which rotates a generator that produces electricity. It was originally designed for the U.S. government by Hamilton Sundstrand for use as a high power lightweight generator.

This apu consists of three major sections: the turbine assembly, reduction drive, and generator. The reduction drive is a system of gears whose purpose is to reduce the high rpm the turbine spins at so the generator can operate. The turbine assembly and electric generator are the main sources or interest.

A. Turbine assembly

A turbine assembly[i] consists of an air compressor, a combustion chamber, and a turbine as shown in Fig. 1. Air enters the compressor, where it is compressed anywhere from 50 to 80 psia. The air is than discharged into a combustion chamber, where fuel is introduced and burned continuously. The compressor and turbine are connected to a common shaft, and the excess power developed by the turbine over the power required by the compressor, is used to run the generator.

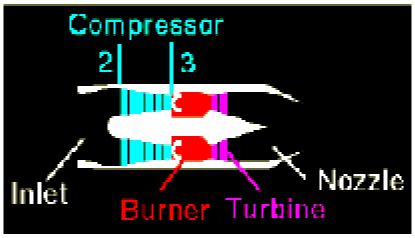

Fig. 1. The turbine assembly.

B. Electric generator

The electric generator consists of a coil that is rotated in the presence of a magnetic field. According to Faraday's law a voltage and thereby current is created. This generator produces three-phase Ac120/208V at 0.75A and a frequency of 400 Hz. Any frequency is acceptable since the negative half of the sinusoidal wave can be inverted by a full wave rectifier to produce DC.

By examining various components of the turbine, studying the existing wiring system and designing a wiring system that will utilize existing relays, sensors and, safety systems it will be determined whether the apu will operate.

A stand was built for the apu so that it could be transported outside and tested more easily (see figure xx). Next existing wires were examined; several had burned through their rubber sleeves and were replaced with ones of heavier gauge. The starter motor was tested, and it functioned properly as did the igniter ignition, inline fuel pump, and cub motor. These tests were encouraging; the gearbox moved freely as did the turbine. Next I followed the fuel from the tank to the cub motor. First the fuel enters a fuel distributor, which is powered by the gearbox and regulated by a diaphragm that senses the pressure in the combustor. After the distributor the fuel is split up into two different lines, a main fuel and a max fuel line. Each line is regulated by electric 3V fuel valves. If the esu detects a problem the valves will close and not open until all the sensors register correct signals. The main valve is continuously open during operation while the max valve is only open during starting times, or when more fuel is needed. After the fuel valves, the lines enter a up side down T-shaped fitting that attaches to the cub motor where the fuel is atomized and blown through the combustor. In the combustor the fuel and air mixture is ignited. The turbine wheel, which is attached to a shaft, harnesses the high-speed exhaust; the shaft is run through a reduction drive gearbox. The turbine assembly has been tested and found to operate well. The generator also functions properly. Before a final test, which will combine all systems, the esu will be bench tested to ensure proper operation. All of the

Figure xx.

sensors through which the esu monitors the apu will also be tested. The fuel system will be purged of air and fresh oil will be added to the reduction drive. A new control panel will be built which will utilize heavy-duty relays to pass current to the starter. With these improvements the apu was run.

Figure xx.

Figure xx through xx shows the stages of the start cycle of the turbine. First in fig xx much smoke and un-burnt fuel can be seen exiting the turbine, this is the only stage environmentally harm full emissions are released. Next the ignition ignites the air fuel mixture (figure xx). After a period of time the starter motor and the ignition are turned off as a fire is continually burning inside of the combustor. As the turbine spins the pressure inside of the gear reduction drive is increased, a higher pitched sound can be heard and the turbine becomes self- sustaining with the entrance of fuel (see figure xx).

Figure xx.

Weights:

W_1 = 225 lb.

W_2 = 225 lb. W_{Front} = 450 lb.

W_3 = 525 lb.

W_4 = 525 lb. W_{Rear} = 1050 lb.

W_{Total} = 1500 lb.

Dimensions:

Front Track (t_F) = 4.67 ft.

Rear Track (t_R) = 4.9 ft

Wheel Base (l) = 8.0 ft.

Center of Gravity Height (h) = 1.0 ft.

Center of Gravity to Roll Axis (H) = .9 ft.

The cornering condition is a left-hand turn where:

α = -10 deg. (roadway bank angle)

R = -600 ft. (radius of the vehicle path, measured horizontally)

V = 80 mph = 117.3 ft./sec.

We assume the following information:

Roll axis heights above ground:

Z_{RF} = 0.25 ft Z_{RR} =0.625 ft

Zero drive torque and longitudinal acceleration:

T_D = 0.0 A_X =0.0

Finally, the following roll rates are assumed:

$K_{\Phi F}$ = 70,000 lb.-ft./rad. = 1222lb.-ft./deg.

$K_{\Phi F}$ = 50,000lb.-ft./rad. = 873 lb.-ft./deg.

First the CG position is determined.

$$b = \frac{W_F l}{W_T} = \frac{450lb \times 8}{1500lb} = 2.4 \text{ ft}$$

a = l-b= 8.0 - 2.4 = 5.6 ft

Next the lateral acceleration values relative to the earth and the banked turn are calculated.

$$A_\alpha = \frac{V^2}{Rg} = -\frac{117.3^2}{-600 \times 32.2} = -0.713\text{g's}$$

$$A_Y = A_\alpha \cos\alpha - \sin\alpha = (-0.713 \times \cos(-10) + \sin(-10))$$

$$= -.7012 - .1737 = 0.876 \text{ g's}$$

Where A_α = Horizontal lateral acceleration

A_Y = Lateral acceleration in car axis system

The effective weight of the car due to banking is

$$W' = W(A_\alpha \sin\alpha - \cos\alpha) = 1500\ (-.713 \sin(-10) + \cos(-10))$$

$$= 1500 \times 1.11 = 1665 \text{ lb}$$

And the effective front and rear axle weights are

$$W_F' = \frac{W'b}{l} = 1665\ \frac{2.4}{8} = 500 \text{ lb.}$$

$$W_R' = \frac{W'a}{l} = 1665\frac{5.6}{8} = 1165 \text{ lb.}$$

The roll gradient is

$$\frac{\Phi}{A_Y} = \frac{-W \times H}{K_{\phi F} + K_{\phi R}} = \frac{-1500 \times 0.9}{70{,}000 + 50{,}000}$$

$$= -0.01125 \text{ rad./g or } -.645 \text{ deg./g}$$

where Φ = body roll angle.

Then the front and rear lateral load transfers due to the lateral acceleration are

$$W_F = A_Y \times \frac{W}{t_F} \times \left(\frac{H \times K_{\phi F}}{K_{\phi F} + K_{\phi R}} + \frac{b}{l} \times Z_{RF} \right)$$

$$W_F = \text{-0.876} \times \frac{1500}{4.67} \times \left(\frac{.9 \times 70{,}000}{120{,}000} + \frac{2.4}{8} \times 0.25 \right)$$

$$W_F = \text{-0.876} \times 321.2 \times (.525 + .075) = \text{-168.82 lb.}$$

$$W_R = A_Y \times \frac{W}{t_R} \times \left(\frac{H \times K_{\phi F}}{K_{\phi F} + K_{\phi R}} + \frac{a}{l} \times Z_{RR} \right)$$

$$W_F = \text{-0.876} \times \frac{1500}{4.9} \times \left(\frac{.9 \times 70{,}000}{120{,}000} + \frac{5.6}{8} \times 0.625 \right)$$

$$W_F = \text{-0.876} \times 306.1 \times (.525 + .4375) = \text{-295.50 lb}$$

Therefore the individual wheel loads are:

Front outside:	W_{FO} = 450/2 + 168.82 = 393.82 lb.
Front inside:	W_{FI} = 450/2 – 168.82 = 56.18 lb.
Rear outside:	W_{RO} = 1050/2 + 295.50 = 820.5 lb.
Rear inside:	W_{RI} = 1050/2 – 295.50 = 229.5 lb.

The change from the static loads measured on level ground are:

Front outside:	W_{FO} = 393.82 - 450 = -56.18 lb.
Front inside:	W_{FI} = 56.18 - 450 = -393.82 lb.

Rear outside: W_{RO} = 820.5 - 1050 = -230 lb.

Rear inside: W_{RI} = 229.5 - 1050 = -820.5 lb.

So next assuming a 3.5 in. of travel available in the suspension, 2.5 in will be used to determine the front and rear suspension rates. Allowing an additional 1 in. for travel due to acceleration and braking.

K_{RF} = 56.18/2.5 = 22.47 lb./in.

K_{RR} = 230/2.5 = 92 lb./in.

Assuming side-to-side symmetry, ride frequencies can be calculated:

$$\omega_F = \frac{1}{2\pi}\sqrt{\frac{K_{RF}\times 12\times 32.2}{W_2}} = \frac{1}{2\pi}\sqrt{\frac{22.47\times 12\times 32.2}{225}} = .99Hz$$

$$\omega_F = \frac{1}{2\pi}\sqrt{\frac{K_{RF}\times 12\times 32.2}{W_2}} = \frac{1}{2\pi}\sqrt{\frac{92\times 12\times 32.2}{525}} = 1.31Hz$$

Total Weight (W_T) = 1500 lb

Wheel Base (l) = 8 ft.

Center of Gravity to Front Axle (a) = 5.6ft

Center of Gravity to Rear Axle (b) = 2.4 ft

The calculations are for coil springs at the front suspensions.

1. Front wheel weight = W = (1/2)(b/l)(W_T) = (1/2)(2.4/8.0)(1500) = 225 lb.
2. A frequency of 2 Hz is chosen as a reasonable un-damped natural frequency for the wheel spring rate.

$\omega = \sqrt{K/m} = 2\pi(2) = 12.56$ rad./sec

Squaring both sides, we have

K= 12.56^2 (225)/ 32.2(12) = 91.9 lb./in.

The relationship between wheel rate and spring rate in a wishbone suspension must next be found. As the linkage ratio is not constant, how the wheel and spring rate relate to each other is given by:

$$K_W = F_S\left(\frac{\Delta IR}{\Delta\delta}\right) + K_S\left(IR\right)^2$$

Where K_W = wheel rate, lb./in.

F_S = spring force, lb.

K_s = spring rate, lb./ in.

IR= installation ratio

Δ IR/ $\Delta\delta$ = change of installation ratio with wheel displacement

As a relation between K_s and K_W desired instaniously change of installation ratio with wheel displacement is zero $\left(\frac{\Delta IR}{\Delta\delta}\right)$ will be zero, leaving the expression:

$$K_W = K_S(IR)^2$$

For this instant a value for (IR) will equal .5 leaving the required spring rate as four times

the wheel rate, or 367.6 lb./in. With G = 11.0$\times 10^6$ psi:

$$S = GD^4 / 8D^3N = 367.6 = 11\times 10^6 d^4 / 8D^3N$$

or $$d^4 / D^3N = 3.342\times 10^{-6} \qquad \text{(a)}$$

The maximum uncorrected stress will be set at 70,000 psi so with:

$$f = 8DW / \pi d^3 = 2.55DW/ d^3$$

$$f = 2.55DW/d^3 = 70{,}000$$

from which

$$D/d^3 = 70{,}000/(2.55 \times \text{static load}) \qquad \text{(b)}$$

and with

$$F_S = W/IR$$

$$D/d^3 = 70{,}000/[2.55 \times (2 \times 225)] = 61 \qquad \text{(c)}$$

With a wire size of qqq, the coil diameter (D) can be calculated form eq. (c) then with d and D input into eq. (a) the minimum number of coils is be found (N).